First-Principles Calculation of Femtosecond Symmetry-Breaking Atomic Forces in Photoexcited Bismuth

Éamonn D. Murray[1,*] and Stephen Fahy[1,2]
[1]Tyndall National Institute, Cork, Ireland
[2]Department of Physics, University College Cork, Cork, Ireland

(Received 25 March 2014; revised manuscript received 5 December 2014; published 4 February 2015)

We present a first-principles method for the calculation of the polarization-dependent atomic forces resulting from optical excitation in a solid. We calculate the induced force driving the E_g phonon mode in bismuth immediately after absorption of polarized light. When radiation with polarization perpendicular to the c axis is absorbed, the photoexcited charge density breaks the threefold rotational symmetry, leading to an atomic force component perpendicular to the axis. We calculate the initial excited electronic distribution as a function of photon energy and polarization and find the resulting atomic force components parallel and perpendicular to the axis. The magnitude of the calculated force is in excellent agreement with that derived from recent measurements of the amplitude of E_g atomic motion and the decay time of several femtoseconds for the driving force.

DOI: 10.1103/PhysRevLett.114.055502 PACS numbers: 63.20.kd, 63.20.dk, 78.20.Ci, 78.47.J-

Understanding the generation and control of atomic forces in optically excited molecules and materials is of importance to a number of areas, including photocatalysis [1], efficient renewable energy, laser annealing of materials, and, increasingly, in furthering our understanding of strongly correlated and charge-density-wave systems [2]. Ultrafast optical spectroscopy has proven to be a powerful tool in the study of structural and electronic dynamics and the effect of optical excitation on materials, with temporal resolution on the tens-of-femtoseconds level readily accessible [3]. More recently, time-resolved x-ray diffraction has allowed us to directly measure the evolution of atomic displacements on a subpicosecond time scale following photoexcitation [4–6]. With such optical and x-ray experimental studies now available, the development of new, quantitative theoretical methods, which can validate proposed mechanisms, is crucial for our understanding of the factors controlling the generation of forces driving atomic motion.

Bismuth has been one of the prototypical materials used in pump-probe reflectivity experiments due to its large vibrational response to optical excitation [7–10]. In particular, high-symmetry coherent A_{1g} phonons can be generated through a mechanism termed displacive excitation of coherent phonons (DECP) [11], which is directly related to the absorptive part of the Raman response [12]. The symmetry-breaking E_g mode has also been detected in these experiments but the mechanism for its generation has been unclear.

The conventional DECP mechanism only generates forces with the full symmetry of the underlying crystal and therefore is not effective in driving atomic motion of E_g symmetry. Zijlstra *et al.* [13] suggested that coherent E_g phonon motion is a result of anharmonic coupling to the DECP-driven A_{1g} mode, although the E_g amplitude estimated by this mechanism is much smaller than that observed. Recent experimental work [7], which measured the decay rate of the force driving the E_g mode in bismuth, found that the E_g force lifetime varies from 13 fs at low temperature to 2 fs at room temperature and suggested that this low-symmetry force may arise from an initial unbalanced occupation of symmetry-equivalent regions in the Brillouin zone, which rapidly decays via electron-phonon scattering to a fully symmetric occupation. A similar conclusion was also reached in recent x-ray diffraction measurements of the E_g mode in bismuth [5], where the magnitude of the atomic displacements associated with the E_g phonon was directly measured.

There have been several theoretical investigations of the DECP mechanism driving the A_{1g} mode in recent years [10,14–16] and all have shown excellent agreement between their density functional theory (DFT) based predictions and experimental measurements despite various approaches to treating the excited electron-hole plasma used in different theoretical studies. However, a quantitative first-principles analysis of the mechanism driving the lower-symmetry E_g mode has thus far been lacking. Because of the very short lifetime of this force, it is clear that the initial optically excited electronic distribution is important, and that the effect of optical polarization and optical transition dipole matrix elements should be accounted for explicitly. Time-dependent DFT based calculations of E_g mode generation have been performed previously [17] for antimony. However, the model optical pulse used in these calculations was more than an order of magnitude higher fluence and significantly shorter duration than that used in the experiment. Moreover, the lifetime of the E_g driving force due to final-state scattering [7] was not

accounted for, leading to results that do not correspond directly to experiment.

In this Letter, we use linear response theory to calculate the driving force on the E_g mode immediately following photoexcitation, demonstrate that the amplitude of atomic vibrations generated is consistent with experimental observations of the force lifetime [7] and amplitude of atomic motion [5], and provide for the first time an understanding of such lower-symmetry forces, based on first-principles electronic structure theory. The method developed here neglects electronic coherence and many-body interactions during the photon absorption process itself, but goes beyond the conventional DECP approach and is applicable to the calculation of atomic forces in a range of molecular and condensed matter systems.

The bismuth unit cell is rhombohedral, with one atom at the origin and a second at a distance zc along the body diagonal (c axis)—see Fig. 1. The internal atomic displacement parameter z is very sensitive to the excitation of electrons to higher bands. This allows for DECP generation of large coherent A_{1g} motion, which corresponds to oscillation of the parameter z. In contrast, the E_g mode corresponds to atomic movement perpendicular to the c axis, which breaks the threefold rotational symmetry of the rhombohedral structure and therefore is not driven by the conventional DECP mechanism.

When photons from an optical pump pulse are absorbed, electrons are excited from the valence bands into the conduction bands, altering the interatomic forces. Because of the dependence of the optical transition matrix elements on the polarization of the electric field $\mathcal{E}$, the photoexcited charge density $\Delta\rho$ and associated atomic forces may have symmetry lower than that of the lattice. As electron-hole pairs are excited by photons from the optical pump, they are continually being scattered due to electron-electron and electron-phonon interaction, leading to rapid decay of the low-symmetry component of the excited carrier distribution and of the corresponding low-symmetry atomic forces [7]. Within this semiclassical framework for the carrier creation and relaxation, the time dependence of the atomic force F can be expressed as

$$\frac{dF}{dt} = \left(\frac{dF}{dt}\right)^{\text{opt}} + \left(\frac{dF}{dt}\right)^{\text{scatt}} = \frac{\partial F}{\partial n^{\text{opt}}}\frac{dn}{dt} - \frac{1}{\tau_F}F, \quad (1)$$

where n^{opt} is the optically excited carrier distribution (in the absence of scattering), $\partial F/\partial n^{\text{opt}}$ is the dependence of the force on n^{opt}, dn/dt is the photon absorption rate, and $1/\tau_F$ is the decay rate of the low-symmetry component of the optically excited distribution due to carrier scattering. We calculate the term $(\partial F/\partial t)^{\text{opt}}$ by constraining the excited distribution of electrons and holes in the system with populations proportional to the (linear) optical absorption in the single-particle approximation [18]:

$$\begin{aligned} R_{n\to m}(\mathbf{k}) &\sim |\langle\Psi_{n\mathbf{k}}|\mathcal{E}\cdot\mathbf{p}|\Psi_{m\mathbf{k}}\rangle|^2\delta[\omega_{m\mathbf{k}} - \omega_{n\mathbf{k}} - \omega] \\ &\equiv |\mathcal{E}\cdot\mathbf{p}_{\text{nm}}(\mathbf{k})|^2\delta[\omega_{m\mathbf{k}} - \omega_{n\mathbf{k}} - \omega], \end{aligned} \quad (2)$$

where $\mathcal{E}$ is the electric field amplitude of the incident radiation at frequency ω, $\mathbf{p}_{\text{nm}}$ is the momentum operator matrix element between bands m and n, $\hbar\omega_{n\mathbf{k}}$ and $|\Psi_{n\mathbf{k}}\rangle$ are the electron energy and eigenstate for the band at momentum $\mathbf{k}$, and δ is the Dirac delta function. The change in electronic density immediately following photon absorption is then proportional to

$$\Delta\rho(\mathbf{r}) \sim \sum_{\text{nm}\mathbf{k}} R_{n\to m}(\mathbf{k})[|\Psi_{m\mathbf{k}}(\mathbf{r})|^2 - |\Psi_{n\mathbf{k}}(\mathbf{r})|^2]. \quad (3)$$

The imaginary part of the linear susceptibility χ [19] gives the band-by-band decomposition of the absorption as a function of photon energy and polarization, which we need to describe the initial photoexcited electronic distribution. This provides details of the bands and k points where electrons and holes will be initially excited for a given incident photon energy and polarization. We have used this to generate explicit occupation numbers for each band and k point, so that the change in occupation of each state following excitation is proportional to the optical absorption to or from that state. These band occupations were then used in a subsequent constrained DFT calculation [20] to find the change in electronic density and the induced forces on the atoms [21].

We performed constrained DFT calculations on bismuth using the ABINIT code package [22]. The calculation of the dielectric function from the OPTIC code was modified to generate the band and k-point decomposition of the absorption needed to describe the excited system [23]. The calculated changes in charge density when 1.5 eV z- or x-polarized photons are absorbed are shown in Fig. 2. The

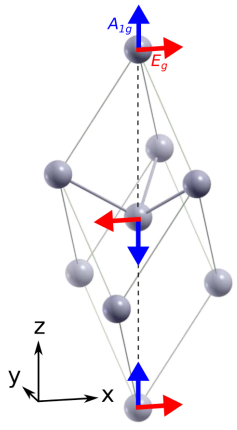

FIG. 1 (color online). The bismuth rhombohedral unit cell. The blue (vertical) and red (horizontal) arrows indicate atomic motion in the z and x Cartesian directions, corresponding to the A_{1g} and E_g phonon modes, respectively. The body diagonal (dashed line) corresponds to the c axis in the text.

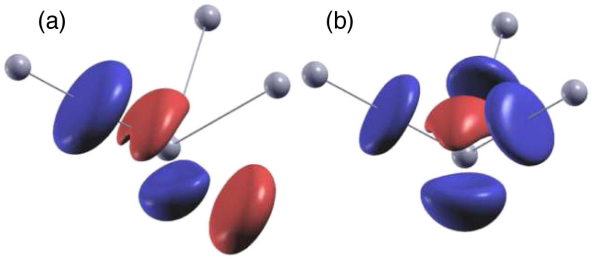

FIG. 2 (color online). The calculated initial change in electronic density when 1% of the valence electrons are excited by 1.5 eV photons polarized in the (a) x direction and (b) z direction. The red (blue) isosurfaces indicate regions where the electron density increased (decreased) by 2×10^{-4} Bohr^{-3}. For clarity, only isosurfaces near the center of the rhombohedral bismuth cell are shown.

breaking of the threefold rotational symmetry by the excited carriers when x-polarized photons are absorbed is clearly visible in Fig. 2(a) [24]. This symmetry breaking leads to a nonzero x component of the atomic force, exciting the E_g phonon mode. (There is also a net force in the z direction, which drives the A_{1g} mode.) In contrast, z-polarized photons lead to a distribution of excited carriers that preserves the threefold symmetry and can only drive the A_{1g} phonon mode [see Fig. 2(b)]. The forces we have calculated as a function of photon energy and polarization (assuming that 0.1 photons are absorbed per unit cell) are shown in Fig. 3. In the linear regime considered here, the

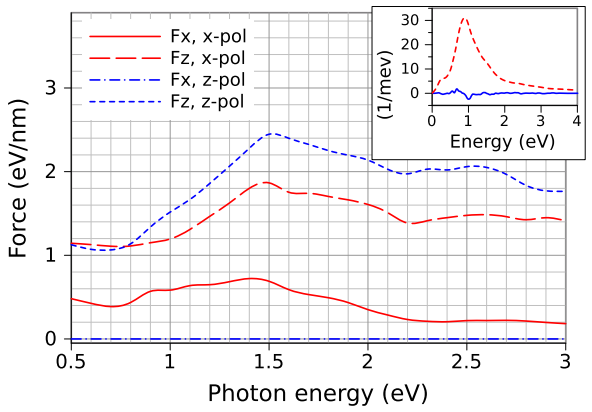

FIG. 3 (color online). The calculated forces on a bismuth atom versus energy of the absorbed photons for both z- and x-polarized photons. The number of photons absorbed is 0.1 per unit cell, corresponding to an excitation of 1% of the valence electrons. The x (z) component of the force is shown as a solid (dashed) line, and red (blue) indicates the polarization of the photons is in the x (z) direction. The inset shows the relative magnitudes of the forces driving the E_g mode due to the real and imaginary parts of ϵ using the expressions from Ref. [25]. The red dashed line shows the contribution from the (absorptive) imaginary part, given by $2i\mathrm{Im}(\epsilon)/(\hbar\Omega)$, and the blue solid line shows the contribution from the real part given by $d\mathrm{Re}(\epsilon)/d\omega/\hbar$. The dominance of the absorptive contribution is clearly visible.

initial atomic forces are proportional to the density of optically excited carriers n^{opt}, so that the values of the force shown in Fig. 3 are equal to $0.1 \times (\partial F/\partial n^{\mathrm{opt}})$ and atomic forces for other densities may be found by scaling the values in Fig. 3.

The forces calculated above are due to optical absorption only, corresponding to the imaginary part of the dielectric function ϵ. In addition, there is in principle a force due to the real part of ϵ, which is present only while the optical radiation is present in the material. The contributions to the phonon driving force due to real and imaginary parts of ϵ are analyzed in Ref. [25]. There it was shown that their relative magnitudes for optical radiation at frequency ω on a phonon of frequency Ω are approximately given by $d\mathrm{Re}(\epsilon)/d\omega$ and $2i\mathrm{Im}(\epsilon)/\Omega$, respectively. These terms are shown in the inset to Fig. 3 for the E_g mode [26]. The dominance of the force due to the imaginary part of ϵ indicates that the force due to optical absorption calculated above dominates over other optical contributions.

In Table I we have compared these forces to those that would be obtained using the DECP occupation schemes employed in previous theoretical studies. Here the "single Fermi-Dirac" occupation refers to the approach used in Refs. [14–16], where the excited electron-hole distribution is represented by occupying the electronic states with a high-temperature Fermi-Dirac distribution. The occupation scheme referred to as "two chemical potential" was used in Ref. [10] and involves representing the excited electrons and holes using a Fermi-Dirac distribution but allowing for different valence and conduction band chemical potentials. The difference in the A_{1g} driving force F_z, as shown in Table I, for 1.5 eV photons is minor between calculations using one or two chemical potentials with Fermi-Dirac occupation of states. We note also that the photoexcited electronic density obtained with both DECP schemes show only minor differences to that shown in Fig. 2(b). However, F_z is substantially larger for both the x- and z-polarized occupations derived from the optical absorption. This demonstrates that there is a significant difference between the initial A_{1g} force and the (smaller) DECP force, to which it decays after electronic relaxation.

We have also calculated the real and imaginary frequency-dependent dielectric function [27] (see Fig. 4). Despite the general limitations of DFT in describing

TABLE I. A comparison of the force on one of the bismuth atoms resulting from different occupation schemes when 1% of the valence electrons are excited to the conduction bands by 1.5 eV photons.

Occupation	F_x (eV/nm)	F_z (eV/nm)
Single Fermi-Dirac	0.00	1.36
Two chemical potential	0.00	1.32
Optical z polarized	0.00	2.45
Optical x polarized	0.69	1.87

conduction band states, and the absence of many-body coherence effects, the agreement between the calculated and measured dielectric function [28] is remarkably good in this case, indicating that the optical absorption properties, i.e., the optical excitation energies and transition matrix elements, are well described in the DFT band structure [29].

The value of $C_{E_g} = (\partial F_{E_g}/\partial n^{\mathrm{opt}})$ can be used with the measured lifetime of the E_g force τ_F from Ref. [7], and the measured decay rate γ_{E_g} of the E_g mode amplitude from Ref. [5], to obtain the amplitude of motion of the atoms when the E_g phonon is excited, which can be compared to the recent x-ray measurements of Ref. [5]. Using the methods in Ref. [32], we simulate the motion of the atoms as a function of depth in the sample, explicitly taking account of the finite duration and penetration depth of the pump pulse and the depth profile and rapid decay of the E_g-symmetry electronic distribution. Details of these calculations are given in the Supplemental Material [33]. This yields a predicted peak measured amplitude of the relative displacements of the atoms in the x direction of 0.28 pm, in very good agreement with the experimental results which show a first maximum of approximately 0.2 pm. Because of the rapid decay of the E_g-symmetry component of the photoexcited carrier distribution, carriers that diffuse into the bulk do not significantly drive the E_g phonon. Hence, we find that the coherent E_g phonon amplitude is significant only within the optical absorption depth. This is in contrast to the A_{1g} phonon amplitude, which is driven by the much longer-lived A_{1g} component of the carrier distribution and does not show the same rapid decay with depth.

The simulation results for the E_g amplitude are well represented if one assumes the initial velocity for the average atomic displacement $\bar{u}_x$, within the x-ray absorption depth z_X is given by

$$\frac{d\bar{u}_x}{dt}(0) = \frac{C_{Eg}\tau_F}{\mu} V_c \frac{\mathcal{F}_{\mathrm{abs}}}{\hbar\omega} (\mathcal{E}\cdot\hat{x})^2 \frac{1}{z_{\mathrm{opt}} + z_X}, \qquad (4)$$

where V_c is the cell volume, $\mathcal{E}$ is the incident polarization, and $\mathcal{F}_{\mathrm{abs}}$ is the absorbed pump fluence, and the subsequent dynamics follow Eq. (12) of Ref. [5] with zero applied force. This gives almost identical results to the full simulation described in the previous paragraph.

In conclusion, we have developed a new, first-principles method for calculating atomic forces in photoexcited materials, which accounts for optical polarization in the absorption process, enabling us to go beyond previous approaches and predict short-lived, lower-symmetry forces that are consistent with experiment. We have shown that the optically excited forces calculated here are consistent with force relaxation times and the amplitudes of motion recently observed for E_g motion in bismuth, thus demonstrating that the mechanism of polarization-dependent electronic excitation investigated here plays a dominant role in driving low-symmetry phonon motion in optically excited materials.

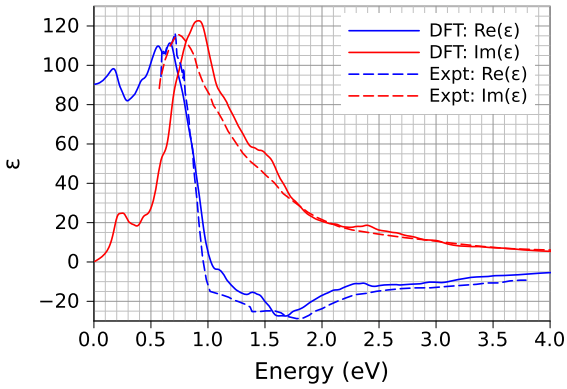

FIG. 4 (color online). The optical dielectric function as a function of frequency for bismuth. The red and blue lines indicate the real and imaginary components of the dielectric function. The solid lines are our isotropically averaged DFT results, with the dashed lines showing the measurements of Ref. [28] on polycrystalline bismuth.

We thank Ivana Savić, David Reis, and Roberto Merlin for helpful discussions. We acknowledge financial support by Science Foundation Ireland under Grant No. 12/1A/1601 and by the EU Commission under Marie Curie International Incoming Fellowship No. 329695.

*eamonn.murray@tyndall.ie

[1] J. Stahler, U. Bovensiepen, M. Meyer, and M. Wolf, Chem. Soc. Rev. **37**, 2180 (2008).
[2] F. Schmitt, P. S. Kirchmann, U. Bovensiepen, R. G. Moore, L. Rettig, M. Krenz, J.-H. Chu, N. Ru, L. Perfetti, D. H. Lu, M. Wolf, I. R. Fisher, and Z.-X. Shen, Science **321**, 1649 (2008).
[3] J. Shah, *Ultrafast Spectroscopy of Semiconductors and Semiconductor Nanostructures* (Springer, Berlin, 1996).
[4] D. M. Fritz *et al.*, Science **315**, 633 (2007).
[5] S. L. Johnson, P. Beaud, E. Möhr-Vorobeva, A. Caviezel, G. Ingold, and C. J. Milne, Phys. Rev. B **87**, 054301 (2013).
[6] M. Trigo *et al.*, Nat. Phys. **9**, 790 (2013).
[7] J. J. Li, J. Chen, D. A. Reis, S. Fahy, and R. Merlin, Phys. Rev. Lett. **110**, 047401 (2013).
[8] T. K. Cheng, S. D. Brorson, A. S. Kazeroonian, J. S. Moodera, G. Dresselhaus, M. S. Dresselhaus, and E. P. Ippen, Appl. Phys. Lett. **57**, 1004 (1990).
[9] M. Hase, M. Kitajima, S.-i. Nakashima, and K. Mizoguchi, Phys. Rev. Lett. **88**, 067401 (2002).
[10] É. D. Murray, D. M. Fritz, J. K. Wahlstrand, S. Fahy, and D. A. Reis, Phys. Rev. B **72**, 060301 (2005).
[11] H. J. Zeiger, J. Vidal, T. K. Cheng, E. P. Ippen, G. Dresselhaus, and M. S. Dresselhaus, Phys. Rev. B **45**, 768 (1992).
[12] R. Merlin, Solid State Commun. **102**, 207 (1997).
[13] E. S. Zijlstra, L. L. Tatarinova, and M. E. Garcia, Phys. Rev. B **74**, 220301 (2006).

[14] Y. Giret, A. Gellé, and B. Arnaud, Phys. Rev. Lett. **106**, 155503 (2011).
[15] E. Papalazarou, J. Faure, J. Mauchain, M. Marsi, A. Taleb-Ibrahimi, I. Reshetnyak, A. van Roekeghem, I. Timrov, N. Vast, B. Arnaud, and L. Perfetti, Phys. Rev. Lett. **108**, 256808 (2012).
[16] J. Faure, J. Mauchain, E. Papalazarou, M. Marsi, D. Boschetto, I. Timrov, N. Vast, Y. Ohtsubo, B. Arnaud, and L. Perfetti, Phys. Rev. B **88**, 075120 (2013).
[17] Y. Shinohara, S. A. Sato, K. Yabana, J.-I. Iwata, T. Otobe, and G. F. Bertsch, J. Chem. Phys. **137**, 22A527 (2012).
[18] O. Madelung, *Introduction to Solid-State Theory* (Springer, Berlin, 1978), pp. 266–269.
[19] J. L. P. Hughes and J. E. Sipe, Phys. Rev. B **53**, 10751 (1996).
[20] P. Tangney and S. Fahy, Phys. Rev. Lett. **82**, 4340 (1999).
[21] Final-state lifetime effects are included by replacing the energy delta function with a Lorentzian, as discussed in Ref. [19]. We use a Lorentzian linewidth of 0.1 eV in calculating $R_{n\to m}$ but find that the calculated initial atomic forces are relatively insensitive to this linewidth.
[22] X. Gonze *et al.*, Comput. Phys. Commun. **180**, 2582 (2009).
[23] These calculations were performed using four shifted $12 \times 12 \times 12$ k-point grids with a Lorentzian broadening, corresponding to an imaginary part of $\hbar\omega$ equal to 0.1 eV. This broadening corresponds approximately to the final-state lifetime inferred from experiment [7] and is somewhat larger than the linewidth of the optical pulses typically used in pump-probe experiments. We used a 15 hartree plane-wave energy cutoff, the local density approximation to exchange and correlation, together with a Hartwigsen-Goedecker-Hutter pseudopotential [35] for bismuth including spin-orbit coupling.
[24] See Supplemental Material at http://link.aps.org/supplemental/10.1103/PhysRevLett.114.055502 for a visual comparison of the distribution of excited electrons in the Brillouin zone for different polarizations.
[25] T. E. Stevens, J. Kuhl, and R. Merlin, Phys. Rev. B **65**, 144304 (2002).
[26] For the A_{1g} mode only Ω changes, leading to the absorptive contribution being approximately 70% smaller but still clearly dominant.
[27] The calculation of the dielectric function was performed using a $32 \times 32 \times 32$ k-point grid, with a Lorentzian broadening of 0.05 eV.
[28] O. Hunderi, J. Phys. F **5**, 2214 (1975).
[29] See Supplemental Material at http://link.aps.org/supplemental/10.1103/PhysRevLett.114.055502 for comparisons of the optical conductivity, reflectivity change with phonon motion, and Raman tensors with previous calculations [30] and experiment [28,31].
[30] H. Katsuki, J. C. Delagnes, K. Hosaka, K. Ishioka, H. Chiba, E. S. Zijlstra, M. E. Garcia, H. Takahashi, K. Watanabe, M. Kitajima, Y. Matsumoto, K. G. Nakamura, and K. Ohmori, Nat. Commun. **4**, 2801 (2013).
[31] J. B. Renucci, W. Richter, M. Cardona, and E. Schöstherr, Phys. Status Solidi B **60**, 299 (1973).
[32] P. Tangney and S. Fahy, Phys. Rev. B **65**, 054302 (2002).
[33] See Supplemental Material at http://link.aps.org/supplemental/10.1103/PhysRevLett.114.055502, which includes Ref. [34], for further details of this simulation and the comparison with x-ray measurements.
[34] Y. M. Sheu, Y. J. Chien, C. Uher, S. Fahy, and D. A. Reis, Phys. Rev. B **87**, 075429 (2013).
[35] C. Hartwigsen, S. Goedecker, and J. Hutter, Phys. Rev. B **58**, 3641 (1998).